

# Differential measurement scheme for Brillouin Optical Correlation Domain Analysis

Ji Ho Jeong,<sup>1,2</sup> Kwanil Lee,<sup>1,4</sup> Kwang Yong Song,<sup>3,\*</sup> Je-Myung Jeong,<sup>2</sup> and Sang Bae Lee<sup>1</sup>

<sup>1</sup>Center for Opto-Electronic Convergence Systems, Korea Institute of Science and Technology (KIST), Seoul 136-791, South Korea

<sup>2</sup>Dept. of Electrical and Computer Engineering, Hanyang University, Seoul 133-791, South Korea

<sup>3</sup>Dept. of Physics, Chung-Ang University, Seoul 156-756, South Korea

<sup>4</sup>klee21@kist.re.kr

\*songky@cau.ac.kr

**Abstract:** We newly propose and experimentally demonstrate a differential measurement scheme for Brillouin optical correlation domain analysis, where the difference between Brillouin gain spectra constructed by a normal and a phase-modulated Brillouin pump waves are analyzed to measure local Brillouin frequencies in optical fibers. In experiments, a five-fold enhancement in the spatial resolution is obtained compared to an ordinary BOCDA system under the same modulation parameters, as a result of the improved dynamic range by the suppression of background noises.

©2012 Optical Society of America

**OCIS codes:** (060.2310) Fiber optics; (060.2370) Fiber optics sensors; (120.5820) Scattering measurements; (290.5900) Scattering, stimulated Brillouin.

---

## References and links

1. X. Bao, D. J. Webb, and D. A. Jackson, "32-km distributed temperature sensor based on Brillouin loss in an optical fiber," *Opt. Lett.* **18**(18), 1561–1563 (1993).
2. M. Nikles, L. Thévenaz, and P. Robert, "Brillouin gain spectrum characterization in single-mode optical fibers," *J. Lightwave Technol.* **15**(10), 1842–1851 (1997).
3. M. N. Alahbabi, Y. T. Cho, and T. P. Newson, "150-km-range distributed temperature sensor based on coherent detection of spontaneous Brillouin backscatter and in-line Raman amplification," *J. Opt. Soc. Am. B* **22**(6), 1321–1324 (2005).
4. K. Hotate and T. Hasegawa, "Measurement of Brillouin gain spectrum distribution along an optical fiber using a correlation-based technique - proposal, experiment and simulation," *IEICE Trans. Electron.* **E83-C**, 405–412 (2000).
5. K. Y. Song, Z. He, and K. Hotate, "Distributed strain measurement with millimeter-order spatial resolution based on Brillouin optical correlation domain analysis," *Opt. Lett.* **31**(17), 2526–2528 (2006).
6. K. Y. Song and K. Hotate, "Distributed fiber strain sensor at 1 kHz sampling rate based on Brillouin optical correlation domain analysis," *IEEE Photon. Technol. Lett.* **19**(23), 1928–1930 (2007).
7. K. Y. Song, M. Kishi, Z. He, and K. Hotate, "High-repetition-rate distributed Brillouin sensor based on optical correlation-domain analysis with differential frequency modulation," *Opt. Lett.* **36**(11), 2062–2064 (2011).
8. K. Y. Song, Z. He, and K. Hotate, "Optimization of Brillouin optical correlation domain analysis system based on intensity modulation scheme," *Opt. Express* **14**(10), 4256–4263 (2006).
9. K. Y. Song, Z. He, and K. Hotate, "Effects of intensity modulation of light source on Brillouin optical correlation domain analysis," *J. Lightwave Technol.* **25**(5), 1238–1246 (2007).
10. J. H. Jeong, K. Lee, K. Y. Song, J.-M. Jeong, and S. B. Lee, "Variable-frequency lock-in detection for the suppression of beat noise in Brillouin optical correlation domain analysis," *Opt. Express* **19**(19), 18721–18728 (2011).
11. K. Hotate, K. Abe, and K. Y. Song, "Suppression of signal fluctuation in Brillouin optical correlation domain analysis system using polarization diversity scheme," *IEEE Photon. Technol. Lett.* **18**(24), 2653–2655 (2006).
12. K. Hotate and H. Arai, "Enlargement of measurement range of simplified BOCDA fiber-optic distributed strain sensing system using a temporal gating scheme," *Proc. SPIE* **5855**, 184–187 (2005).
13. K. Y. Song and K. Hotate, "Enlargement of measurement range in a Brillouin optical correlation domain analysis system using double lock-in amplifiers and a single-sideband modulator," *IEEE Photon. Technol. Lett.* **18**(3), 499–501 (2006).
14. J. H. Jeong, K. Lee, K. Y. Song, J.-M. Jeong, and S. B. Lee, "Bidirectional measurement for Brillouin optical correlation domain analysis," *Opt. Express* **20**(10), 11091–11096 (2012).

## 1. Introduction

Distributed fiber sensors based on stimulated Brillouin scattering (SBS) have been regarded as an efficient tool for temperature or strain measurement in the health monitoring of various civil structures and materials [1–4]. Among different types of the Brillouin sensors so far demonstrated, Brillouin optical correlation domain analysis (BOCDA) can provide an easiest way to realize a high spatial resolution of an order of mm and a high sampling- or repetition-rate by the operation of frequency-modulated pump and probe waves [5–7]. A BOCDA system basically works as a point sensor with random accessibility of the sensing position (called ‘correlation peak’) with the measurement range limited by a half-period of the frequency modulation. In principle, the measured signal of a BOCDA system is the spatial sum of the spectral convolution between an local Brillouin gain spectrum (BGS) and a local pump-probe beat spectrum, which appears to be an addition of a sharp and Lorentzian-shaped BGS from the correlation peak (i.e. sensing position) and a broad noise structure of an trapezoid shape stacked from all the other positions. This feature restricts the dynamic range (i.e. the maximum value of Brillouin frequency shift) of distributed measurements [8]. In previous works, an intensity modulation has been introduced for the suppression of the noise structure by an active and delicate control of the pump-probe beat spectrum at the cost of additional complexity in the system [8,9].

In this paper, we newly propose a differential measurement scheme for the BOCDA, where the difference between the BGS constructed by a normal and a phase-modulated Brillouin pump waves is analyzed to measure local Brillouin frequencies ( $\nu_B$ ) of optical fibers. Our experiments show that the differential measurement, implemented by a simple modification in the lock-in detection of the BOCDA, can effectively suppress the noise structure of the signal, and lead to potentially unlimited dynamic range in the measurement of the  $\nu_B$ . As another result of the noise suppression, it is demonstrated that the spatial resolution is improved by as much as five times compared to ordinary BOCDA systems under the same modulation parameters. In experiments, the measurement of the  $\nu_B$  of a 2 cm fiber section is successfully performed by the differential measurement under a nominal spatial resolution of 10 cm, as well as the confirmation of the noise suppression resulting in the improvement of the dynamic range.

## 2. Principle

When a sinusoidal frequency modulation is applied to counter-propagating pump and probe waves in the BOCDA, the beat frequency  $f_B$  between these two waves is given by the following equation [9]:

$$f_B(\Delta x, t) = \Delta\nu + 2\Delta f \cdot \sin(2\pi f_m \cdot \frac{\Delta x}{V_g}) \cdot \cos(2\pi f_m (t - \frac{\Delta x}{V_g})) \quad (1)$$

where  $\Delta\nu$ ,  $\Delta f$ ,  $f_m$ , and  $V_g$  are the frequency offset, the modulation amplitude, the modulation frequency, and the group velocity of the light wave, respectively.  $\Delta x$  is the propagation length difference between pump and probe waves. The BOCDA signal is composed of the spatial sum of the convolution between the local spectrum of  $f_B$  and a local BGS along the fiber. As shown in Fig. 1(a), at a correlation peak (CP), the sine term in Eq. (1) vanishes and the beat spectrum becomes a  $\delta$ -function adding a sharp and Lorentzian-shaped BGS to the BOCDA signal. As  $\Delta x$  is away from the correlation peak, the local spectrum of  $f_B$  starts to broaden, contributing to the noise structure of the BOCDA signal. In this way, the BOCDA signal is constructed by the BGS from a CP and a trapezoid noise structure from all the other sections of a fiber under test (FUT) as depicted in Fig. 1(b).

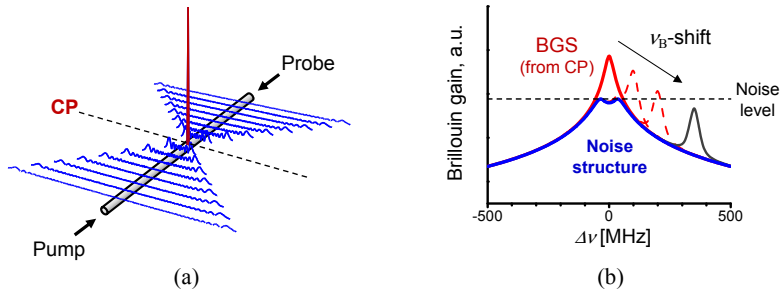


Fig. 1. (a) Distribution of a pump-probe beat spectrum near a correlation peak (CP) in the BOCDA. (b) Structure of a BOCDA signal composed of a sharp BGS from the CP (red) and a noise structure (blue) from other sections of a fiber under test.

The specific shape of the noise structure practically limits the dynamic range of the measurement as shown in Fig. 1(b), where the proper detection of the  $\nu_B$  fails (gray) if the noise level becomes larger than the BGS peak from the CP due to a large shift of  $\nu_B$ . The dynamic range of ordinary BOCDA system is known to be about 230 MHz when the shift of  $\nu_B$  takes place within the span of the nominal spatial resolution [9].

For the suppression of the noise structure we newly propose a differential measurement scheme. As schematically shown in Fig. 2(a), the ordinary BOCDA signal (Signal1) is constructed by the spatial sum of the convolution between a local BGS of a Lorentzian shape and a local beat spectrum between the pump and the probe. If a phase modulation of a frequency  $\Omega$  ( $\Delta f \gg \Omega$ ) is additionally applied only to the pump for carrier suppression and spectral broadening, the local BGS is spread out as depicted in Fig. 2(b) (Local BGS2). This implementation leads to a different BOCDA signal (Signal2) with the sharp BGS peak removed. It is notable that such a broadening effect by the phase modulation is the largest at the CP and becomes negligible at which the beat spectrum is already broad. Therefore Signal2 shares a similar noise structure with Signal1, and one can obtain a specific BOCDA signal composed only of a sharp BGS by analyzing the difference between Signal1 and Signal2 as shown in Fig. 2(c). As a result of the removal of the noise structure, it is expected that the measurements of  $\nu_B$  do not suffer from the limited dynamic range, which could eventually lead to the enhancement of the spatial resolution. Theoretically, the spatial resolution of the BOCDA is defined as the span where the full width of the beat spectrum broadens twice as wide as the Brillouin gain bandwidth ( $\Delta\nu_B \sim 30$  MHz in optical fibers) considering the suppressed level of the Brillouin signals at the positions near the CP, which is expressed by the following equation [4]:

$$\Delta z_r = \frac{V_g \cdot \Delta\nu_B}{2\pi \cdot f_m \cdot \Delta f} \quad (2)$$

Since the differential measurement provides a strong suppression of the Brillouin signals at the positions except the CP, one can expect a large enhancement of the spatial resolution compared to the nominal value given by Eq. (2).

Another practical advantage of the differential measurement is that it can be easily implemented by simple modification of a lock-in detection applied for the signal processing of ordinary BOCDA systems [4, 10]. If the phase modulation is applied to the pump with an on-off control operated at  $f_L$ , one can obtain the result of the differential measurement directly from the output of a lock-in amplifier with a reference frequency of  $f_L$ . Figure 2(d) shows the amplitude modulated RF wave which is applied to the phase modulator (PM) of the pump for the differential measurement. It is implemented by 100% modulation of a sine wave by square binary wave.

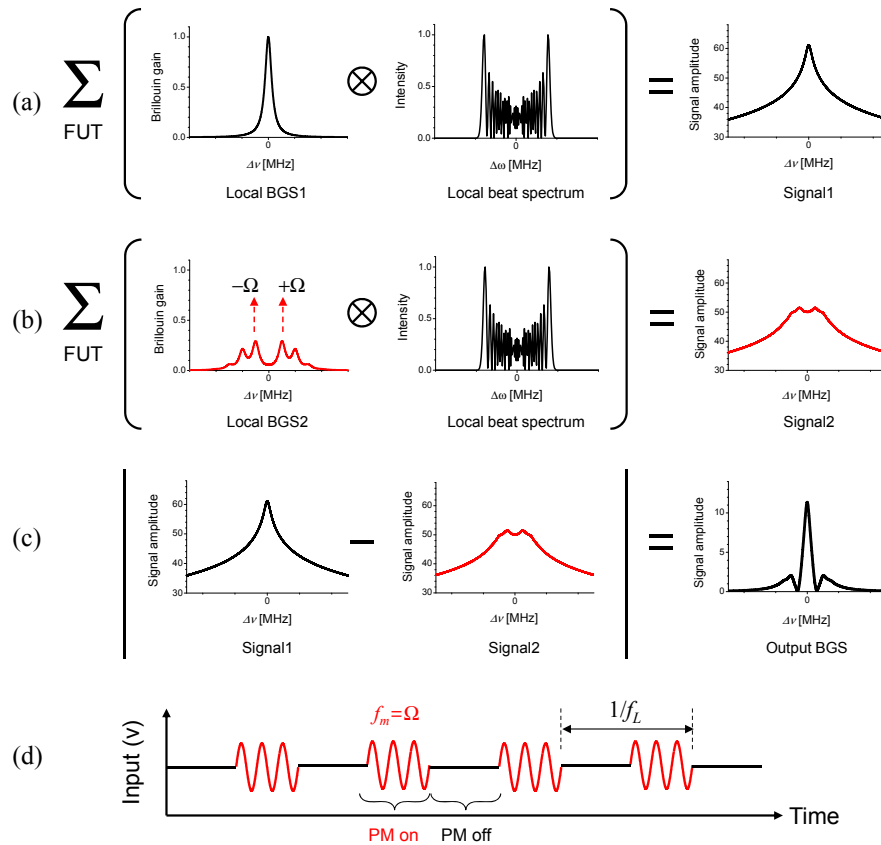


Fig. 2. (a) Construction of a BOCDA signal (Signal1) with an ordinary pump wave. (b) Construction of a BOCDA signal (Signal2) with a phase-modulated pump wave. (c) Differential measurement by analyzing the difference of Signal1 and Signal2. (d) An RF wave input to the phase modulator for the pump in the differential measurement.

### 3. Experimental results

The experimental setup for a BOCDA system based on the differential measurement is shown in Fig. 3. A 1550 nm distributed feedback laser diode (DFB-LD) was used as a light source where a frequency modulation ( $\Delta f \sim 5$  GHz,  $f_m = 1.9$  MHz) is applied for the synthesis of optical coherence function. The modulation parameters correspond to a nominal spatial resolution of about 10 cm by Eq. (2) and a measurement range of 54 m [4]. The output of the LD was divided into two beams by a 3-dB coupler. One of them was injected into a single-sideband modulator (SSBM) driven by a microwave sweep generator where the lower sideband output ( $\nu_0 - \Delta\nu$ ) was utilized as a probe wave. The other beam was amplified by an Erbium-doped fiber amplifier (EDFA) after propagating a 10 km delay fiber, to be used as the pump. In order to apply the differential measurement, a phase modulator was used for the pump with  $\Omega = 5$  MHz and the driving voltage periodically on and off at the lock-in frequency ( $f_L = f_m / 4$ ) as depicted in Fig. 2(d) [10]. The pump and the probe were launched into a 50 m FUT through a circulator and an isolator, respectively, in opposite direction to each other. In addition, a polarization switch (PSW) was inserted after the SSBM for compensating the polarization dependence of the Brillouin gain [11]. The probe signal was detected by a 125 MHz photo detector (PD) connected to a lock-in amplifier for the signal processing.

The BGS of a single position was obtained by sweeping the frequency of the microwave generator in the vicinity of the Brillouin frequency, and distributed measurements along the FUT were carried out by varying  $f_m$ . The FUT was prepared by concatenating single-mode fibers (SMF's) and 8 pieces of dispersion-shifted fibers (DSF's) with different lengths representing 1.5, 1.2, 1, 1/2, 1/3, 1/4, 1/5, 1/10 times of the spatial resolution, shown in the inset of Fig. 3. The  $\nu_B$  was about 10.87 for the SMF and 10.52 GHz for the DSF, respectively.

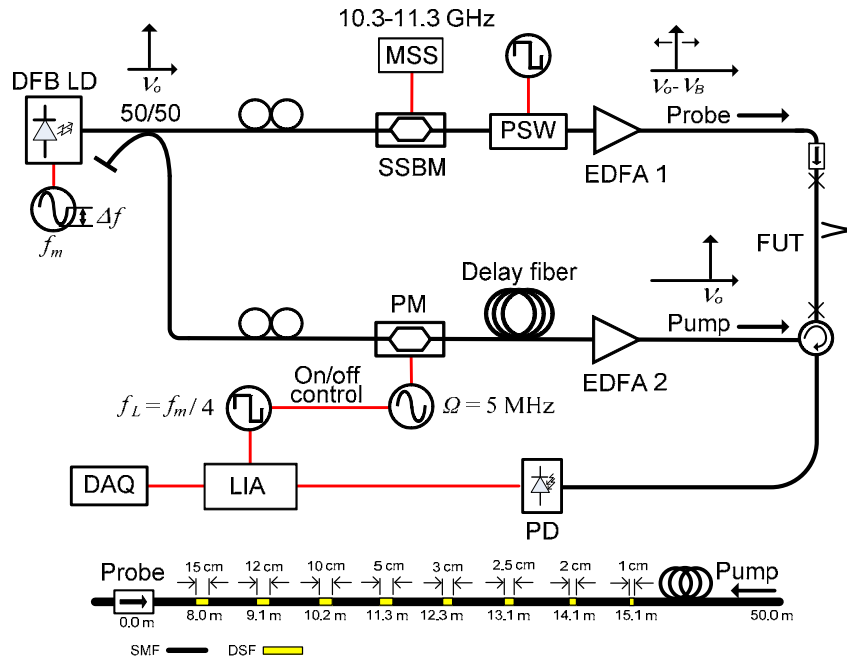


Fig. 3. Experimental setup for a BOCDA system based on the differential measurement. The inset shows the structure of a 50 m FUT composed of SMF's and eight sections of DSF with different lengths: SSBM, single-sideband modulator; MSS, microwave sweep synthesizer; PSW, polarization switch; EDFA, Er-doped fiber amplifier; PM, phase modulator; LIA, lock-in amplifier.

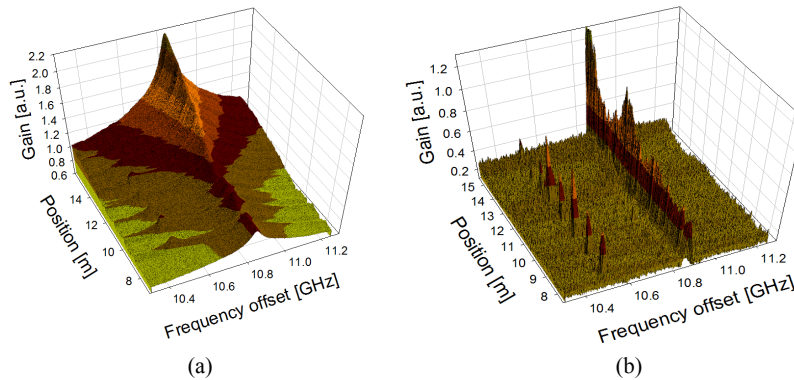


Fig. 4. 3D plots of BOCDA signals by (a) an ordinary setup and (b) the differential measurement scheme.

In order to confirm the effects of the differential measurement, we performed distributed measurements of  $\nu_B$  with two different schemes; one with an ordinary BOCDA and the other with the differential measurement scheme. Additionally, a signal to noise ratio (SNR) defined as the amplitude ratio of the signal peak to the noise peak in BOCDA signals is used for the

evaluation of the suppression of noise structure. Figure 4 shows the 3D plots of the measurement results, where one can clearly see the overall suppression of the noise structure in the differential measurement (b) compared to the ordinary case (a). The attenuation of the signal dominantly seen in Fig. 4(a) is due to the splice loss of the FUT.

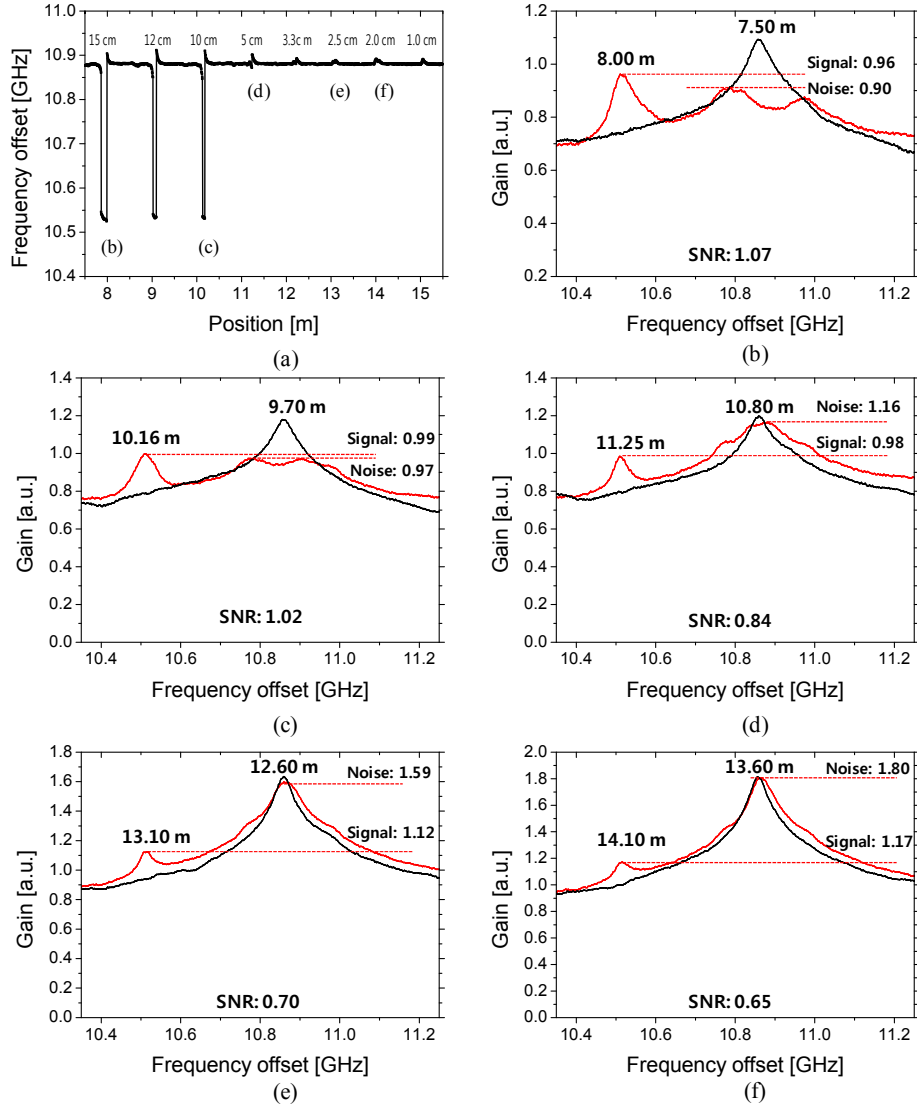


Fig. 5. (a) Distribution map of  $\nu_B$  measured by the ordinary BOCDA. (b)-(f) The BOCDA signal at each section of the DSF (red) plotted together with that of a SMF section (black).

Figure 5 shows the distribution map of  $\nu_B$  and the BOCDA signals at five different DSF sections (red) compared to that of SMF (black) by the ordinary BOCDA setup. As expected by the nominal spatial resolution of 10 cm, the measurement was successful to the barely measured 10 cm DSF section with an SNR of 1.02, and the measured  $\nu_B$ 's are not correct at the shorter sections of the DSF. This result is attributed to the noise structures higher than the signal level as apparently shown in Fig. 5(d)-(f) with SNR's less than 1.

Meanwhile, in the BOCDA based on the differential measurement, the distribution of  $\nu_B$  is successfully measured even to a 2 cm section of the DSF as shown in Fig. 6(a). As also observed in Fig. 6(b)-(e), the spectral width of the signal is much smaller than that of the ordinary system, comparable to the intrinsic gain bandwidth of SBS ( $\sim 30$  MHz) with almost complete suppression of the noise structure appearing in Fig. 5. It is also noticeable that the limitation of the dynamic range is effectively removed by the ‘flat’ background. According to this result, it is confirmed that at least a 2 cm spatial resolution is achieved based on the differential measurement, which is 5 times better than that of the ordinary BOCDA system.

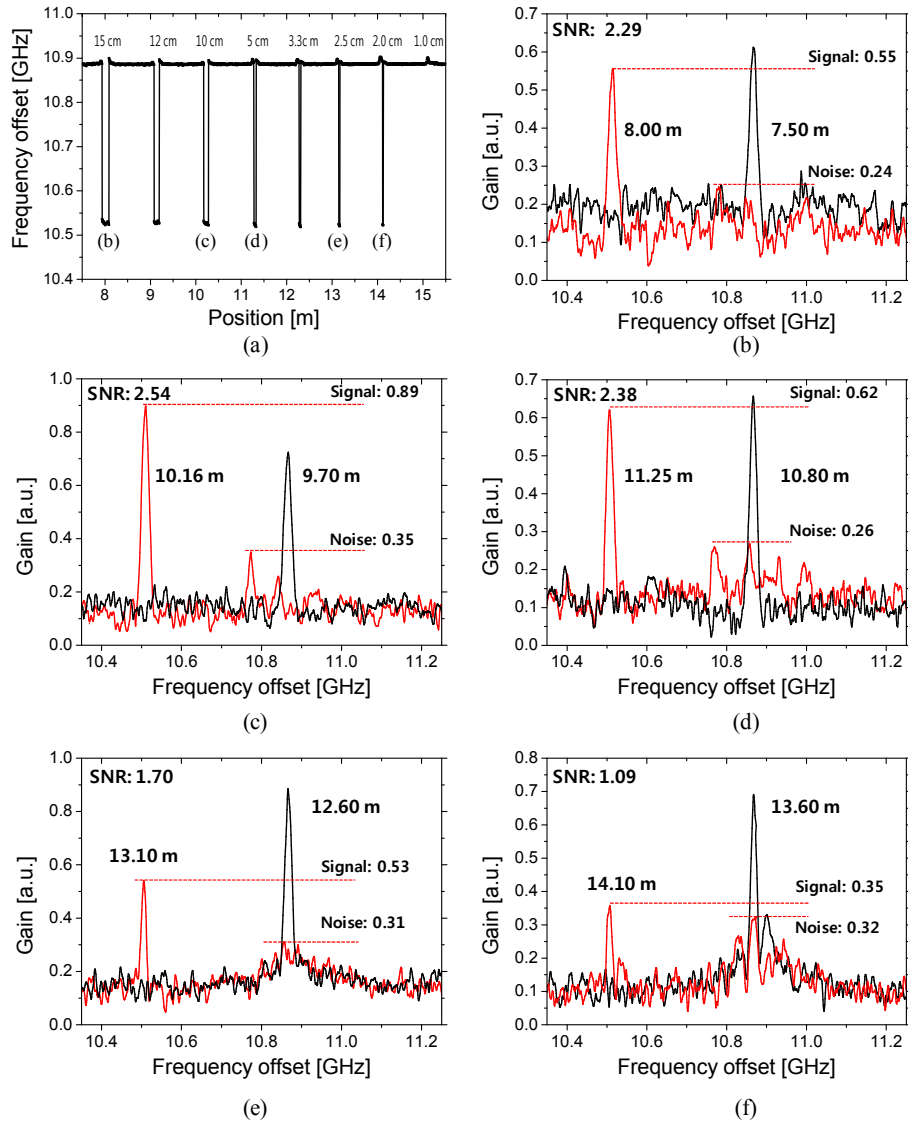


Fig. 6. (a) Distribution map of  $\nu_B$  measured by the BOCDA system based on differential measurement. (b)-(f) The BOCDA signal at each section of the DSF (red) and the SMF (black).

#### 4. Conclusion

We have proposed and experimentally confirm the differential measurement for the BOCDA system, which provides the suppression of noise structure and the enhancement of both the dynamic range and the spatial resolution. We think this approach could be implemented also by an intensity modulation in a similar way to the phase modulation, and the analytic formulation and optimization of the operation condition would be possible for further studies. It should be noted that the suppression of the noise structure is also accompanied by certain degree of the signal suppression, and the differential measurement can be considered as another effective tool for the range enlargement of the BOCDA [12–14], since the improvement of the spatial resolution means as much increase of the effective number of sensing points [13]. We think the dynamic range of the proposed scheme is currently limited only by the span of  $\Delta\nu$  sweep of the microwave sweeper. In BOCDA systems, the span is usually set to 1 GHz corresponding to  $\pm 1\%$  strain, which may be enough for most applications in structural health monitoring, and also easily expandable when necessary.

#### Acknowledgment

This work was partially supported by Basic Research Program through the National Research Foundation of Korea (NRF) funded by the Ministry of Education Science and Technology (2012-0005397).